Enzyme/NanoCopper hybrids Nanozymes: Modulating Enzyme-like Activity by the protein structure for biosensing and tumor catalytic therapy

Noelia Losada-Garcia,[1] Ana Jimenez-Alesanco,[3] Adrian Velazquez-Campoy,[2-6] Olga Abian[3-7] and Jose M. Palomo[1]*

[1]Department of Biocatalysis, Institute of Catalysis (CSIC)

Address: c/marie curie 2, cantoblanco campus UAM, 28049, Madrid, Spain

e-mail: josempalomo@icp.csic.es

[2] Fundación ARAID, Gobierno de Aragón, Zaragoza, Spain;

[3]Instituto de Biocomputación y Física de Sistemas Complejos, Joint Units IQFR-CSIC-BIFI, and GBsC-CSIC-BIFI, Universidad de Zaragoza, Spain

[4]Fundación Instituto de Investigación Sanitaria de Aragón (IIS Aragón), Zaragoza, Spain

[5]Centro de Investigación Biomédica en Red en el Área Temática de Enfermedades Hepáticas y Digestivas (CIBERehd), Madrid, Spain

[6]Departamento de Bioquímica y Biología Molecular y Celular, Universidad de Zaragoza, Zaragoza, Spain

[7]Instituto Aragonés de Ciencias de la Salud (IACS), Zaragoza, Spain

Abstract

Artificial enzymes with modulated enzyme mimicking activities of natural systems represent a challenge in catalytic applications. Here we show the creation of artificial Cu metalloenzymes based on the generation of Cu nanoparticles in an enzyme matrix. Different enzymes were used and the structural differences between the enzymes especially influenced the controlled of the size of the nanoparticles and the environment that surrounds them. Herein, we demonstrated that the oxidase-like catalytic activity of these copper nanozymes was rationally modulated by enzyme used as scaffold, with a special role in the nanoparticle size and their environment. In this sense, these nanocopper hybrids has confirmed the ability to mimic a unique enzymatic activity completely different that the natural activity of the enzyme used as a scaffold, such as tyrosinase-like activity or as Fenton catalyst, which has extremely higher stability than natural mushroom tyrosinase. More interestingly, the oxidoreductase-like activity of nanocopper hybrids was cooperatively modulated with the synergistic effect between the enzyme and the nanoparticles improving the catalase activity (no peroxidase activity). Additionally, a novel dual (metallic and enzymatic activity) of the nanozyme allowed to highly improved cathecol-like activity interesting for the design of L-DOPA biosensor for detection of tyrosinase. These hybrids also showed cytotoxic activity against different tumor cells, interesting in biocatalytic tumor therapy.

Keywords: nanozymes, copper hybrids, nanoparticles, oxidase-like activity, biosensors, cytotoxicity.

1. Introduction

One of the key advantages of enzymes is the high selectivity and activity against a particular reaction, however, outside of cells they present low activity against non-natural substrate and low stability in different media than biological environment, which are important drawbacks for commercial applications. Also, difficult and time-consuming purification steps who are translated in a final high cost of the product limit their industrial application.

Nanozymes have emerged in the last years as one of the most interesting alternatives to natural enzymes, and even conventional enzyme mimics, as artificial biocatalytic tools for decontamination, biosensor and biomedical applications.[1-14]

At this point, the nanozymes represent unique advantages over natural enzymes offering robustness to harsh environments, high stability, long-term storage, ease of modification and lower manufacturing cost than protein enzymes. Additionally, nanozymes possess inherent nanomaterial properties, providing not only a simple substitute of enzymes but also a multimodal platform interfacing complex biologic environments.[3,15-16]

However, one of the most challenge actually is the development of novel strategies to synthesize nanozymes which mimic a particular natural activity, specially being able for specific enzymatic activity that has not been studied much.

Most of the currently developed nanozymes still face several challenges such as limited specificities and catalytic activities when compared with their natural counterparts.[17-18] To bypass these challenges, several strategies based on the functionalization of nanozymes surface or designing novel nanozymes with structures similar to the active site of natural enzymes have been described.[19-20]

Thus, creating new activities competitive respect to natural enzymes, with improved stability or even founding synergistic processes between enzyme and metallic catalytic centers[21-23] are challenging.

In particular, mimics of copper metalloenzymes is an important case, considering the essential biological role of these enzymes.[24-28] Phenol oxidases (catechol oxidases, tyrosinases), catalases, superoxide dismutase activities are involved in many different cellular process and deficiency or malfunction of these activities is postulated to be related to the pathogenesis of many age-associated degenerative diseases like diabetes mellitus, hypertension, anemia, vitiligo, Alzheimer's disease, Parkinson's disease, bipolar disorder, cancer, and schizophrenia.[29-33]

Here in this work we demonstrate how to modulate the particular enzyme-like activity of a novel copper nanohybrids, formed by copper nanoparticles (as active sites) created in a protein environment (as scaffold), where precisely the used enzyme plays a fundamental role.

Here we found that depending on the enzyme used in the synthesized hybrid (Figure 1), it was possible to obtain Cu nanozymes with a modulate-activity by altering the nanoparticle morphology and reactivity. For that purpose, enzymes with different nature, behaviors and size were tested, with the ability to mimics a particular enzyme activity completely different that the natural activity of the enzyme used as scaffold, the highest tyrosinase-like activity or even other oxidase activity in Fenton processes,[34] for catalysis for example applied in biocatalytic tumor therapy.[35-36]

Furthermore, a synergistic effect between the enzyme as scaffold and the CuNPs was observed to an enhanced catalase activity.

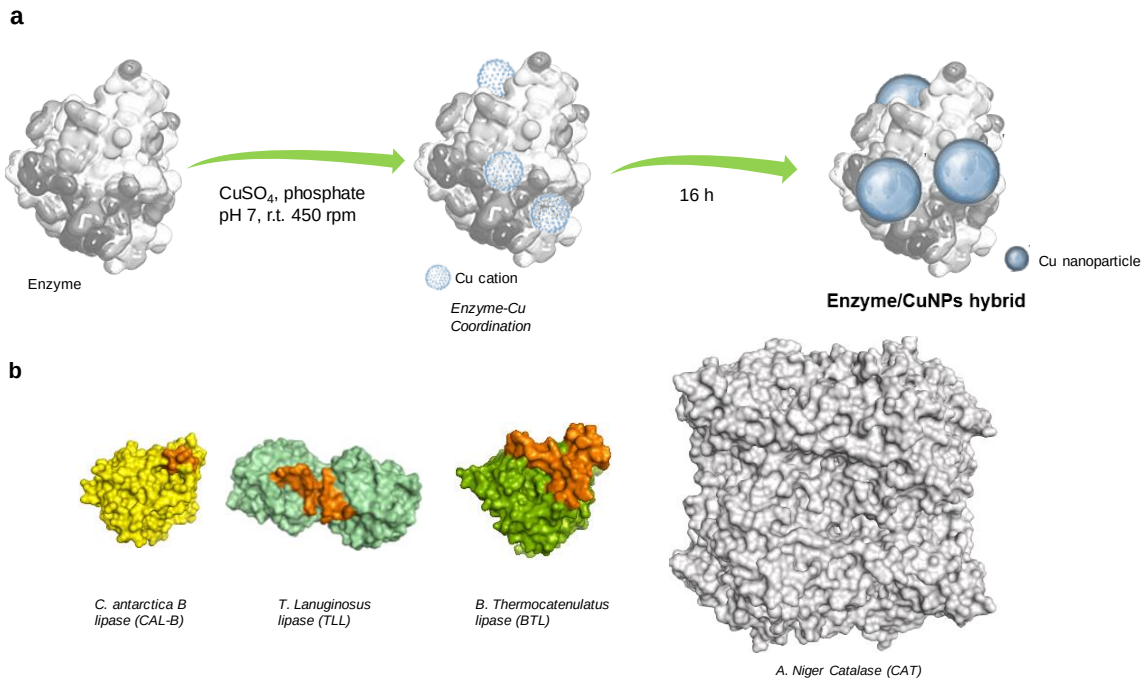

Figure 1. **General Concept and Design of Enzyme/CuNPs hybrids as novel nanozymes.** (a) Synthetic Strategy. (b) Different enzymes used as protein scaffold (orange colour represent the oligopeptide lid in lipases).

2.Experimental Section

2.1 Chemicals

Lipase B from *Candida antarctica* (CALB) solution (Lipozyme® CALB), lipase from *Thermomyces lanuginosus* solution (Lipozyme® TL 100L), Catalase from *Aspergillus niger* (CAT) solution (Catazyme®) and glucose oxidase (Gluzyme® Mono 10.000 BG) (GOX) were purchased from Novozymes (Copenhagen, Denmark). Genetically modified lipase from (*Geo)bacillus Thermocatenulatus* without native cysteines (C65S/C296S) BTL) was produced by Dr. de las Rivas and purified following the previous report (obtaining a solution of 2.5 mg lipase/mL by Bradford assay determination).[37] Copper (II) sulfate pentahydrate [Cu_2SO_4 x $5H_2O$] and hydrogen peroxide (33%) were from Panreac (Barcelona, Spain). P-aminophenol (pNP), sodium phosphate, sodium acetate, tyrosinase from mushroom (TYR), 2,2′-Azino-bis(3-ethylbenzothiazoline-6-sulfonic acid) diammonium salt (ABTS), benzoquinone, hydroquinone were purchased from Sigma-Aldrich (St. Louis, MO, USA). 3,4-Dihydroxy-L-phenylalanine (L-DOPA) was from Alfa Aesar (Massachusetts, EEUU). 3,4-Dihydroxy-L-phenylalanine methyl ester hydrochloride (L-DOPA methyl ester) from Carbosynth (Berkshire, UK). Horseradish peroxidase (HRP) was from Thermo Scientific (Madrid, Spain).

2.2 Instrumentation

Cu nanoparticles sizes and morphology were determined by Transmission electron microscopy (TEM) and high resolution TEM microscopy (HRTEM). Images were obtained on a 2100F microscope (JEOL, Tokyo, Japan) equipped with an EDX detector INCA x-sight (Oxford Instruments, Abingdon, UK). Interplanar spacing in the nanostructures was calculated by using the inversed Fourier transform with the GATAN digital micrograph program (Corporate Headquarters, Pleasanton, CA, USA). Scanning

electron microscopy (SEM) imaging was performed on a TM-1000 microscope (Hitachi, Tokyo, Japan). Inductively coupled plasma - optical emission spectrometry (ICP-OES) was performed on a OPTIMA 2100 DV instrument (PerkinElmer, Waltham, MA, USA). X-Ray diffraction (XRD) patterns were obtained using a Texture Analysis D8 Advance Diffractometer (Bruker, Billerica, MA, USA) with Cu Kα radiation. To recover the nanobiohybrids, a Biocen 22 R (Orto-Alresa, Ajalvir, Spain) refrigerated centrifuge was used. Spectrophotometric analyses were run on a V-730 spectrophotometer (JASCO, Tokyo, Japan). Synergy HT (BioTek) plate reader was used for cell viability assays.

2.3 General synthesis of Enzyme-Cu(II)NPs hybrids

A corresponding amount of enzyme was added to 60 mL sodium phosphate buffer 0.1M pH=7 in order to finally achieved an enzyme concentration of 0.27-0.3 mg/ml. In the case of CALB solution, 1.8 ml (9 mg lipase/mL determined by Bradford assay) were added. 0.75 mL of TLL solution (24 mg/ml determined by Bradford assay) and 0.5 mL of CAT (32 mg/mL determined by Bradford assay) were added respectively. In the case of BTL, 20 ml (0.4 mg/mL solution containing 0.5% (w/v) of Triton X-100 from the purification step) were added, corresponding to an enzyme concentration of 0.13 mg/ml. The corresponding enzyme solution was poured in a 100 mL glass bottle containing a small magnetic bar stirrer (12x4.5 mm). The solution was stirring in a magnetic agitator at 380-450 r.p.m. for 1-2 min. Then, 600 mg of Cu_2SO_4 x $5H_2O$ (10 mg/ml) was added to the protein solution and it was maintained for 16 hours at room temperature. After that, in all cases, the mixture was centrifuged at 8000 rpm for 5 min, (10 mL per falcon type tube). The generated pellet was re-suspended in 15 mL of water, washed and centrifuged again at 8000 r.p.m for 5 min and the supernatant removed. The process was repeated twice more. Finally, the supernatant was removed and the pellet of each falcon was re-

suspended in 2 mL of water, collected each solution in a cryotube, frozen with liquid nitrogen and lyophilized for 16 hours. After that, in all cases, approximately 350 mg of a blue solid were obtained. The different hybrids were called as **Cu-CALB, Cu-TLL, Cu-CAT** and **Cu-BTL**. In the case of CAT, the protocol was repeated avoiding the lyophilization step, conserving the catalyst as a blue liquid suspension. This was called **Cu-CAT-NL**. Characterization of the different Cu hybrids was performed by XRD, SEM, TEM, HRTEM, CD and fluorescence analysis.

2.4 Circular dichroism measurements

Circular dichroism (CD) spectra of the different lipases were recorded in a Chirascan spectropolarimeter (Applied Photophysics) at 25(±1)°C. Far-UV spectra were recorded at wavelengths between 190 and 260 nm in a 0.1 cm path-length cuvette. Near-UV spectra were recorded at wavelengths between 250 and 310 nm in a 1 cm path-length cuvette. Protein concentrations were 20 and 10 μM respectively in phosphate buffered saline, pH 7.2 (PBS; bioMerieux).

2.5 Fluorescence spectroscopy measurements

Fluorescence measurements were performed in a Varian Cary Eclipse Fluorescence Spectrophotometer (Agilent Technologies) monitoring the intrinsic tryptophan fluorescence in 2 μM of hybrid solutions, using an excitation wavelength of 280 nm, with excitation and emission bandwidths of 5 nm, and recording fluorescence emission spectra between 300 and 400 nm with 1 nm step. All spectroscopic measurements were made in water.

2.6 Tyrosinase-like activity assay

3,4-Dihydroxy-L-phenylalanine (L-DOPA) (4 mg, 1mM) or L-DOPA methyl ester (5 mg, 1mM) was added to a 20 mL water solution, 0.1M buffer sodium phosphate pH 7 or 0.1M buffer sodium acetate pH 4. To initialize the reaction, 5 mg of Cu-enzyme hybrid or 50 µL of commercial mushroom tyrosinase (TYR) (1mg/mL solution in distilled water) were added to 2 mL of DOPA solution and the mixture was slight stirred (roller) at room temperature. In the case of solid Cu hybrids, at different times the mixture was centrifuged at 3000 rpm for 1 min and the absorbance of supernatant (at different times) was measured at 475 nm in a JASCO V-730 UV-spectrophotometer. Then, the Abs/min was calculated with these values in each case. In the case of tyrosinase, the increase of absorbance was directly measured at 475 nm the UV spectrophotometer using the kinetic programme. An enzyme activity Unit (U) was defined as the amount of enzyme causing an increase of absorbance by 0.001/min at 25ºC.[38] Experiments were also made in the presence of different concentrations of H_2O_2 (0-50 mM).

2.7 Catalase-like activity assay

Hydrogen peroxide (H_2O_2) (33%(w/w) solution in distilled water was prepared in order to obtaining a final concentration of 50 mM. The solution pH was adjusted to 7 using NaOH. To start the reaction, 2 mg of the Cu hybrid or 100 µL of Catazyme® 25L (31 mg/mL) was added to a 2 mL or 10 mL respectively of the 50 mM solution at room temperature. The reaction was followed by measuring the degradation of hydrogen peroxide recording the decrease of absorbance by spectrophotometrically at 240 nm in quartz cuvettes of 1 cm path length, at different times. In order to determine the catalase activity for each catalyst, the ΔAbs/min value was calculated using the linear portion of the curve (ΔAbs_S).

The specific activity (U/mg) was calculated using the following equation:

$$U(\mu mol \cdot min^{-1} \cdot mg^{-1}) = \Delta Abs/\min \cdot V \cdot \frac{1000}{\varepsilon \cdot mg_{catalyst}}$$

where the molar extinction coefficient (ε) used was 43.6 $M^{-1}cm^{-1}$, and mg of enzyme or cu content.

2.8 Fenton catalyst assay

p-aminophenol (pAP) (1 mg) was dissolved in solutions (10 mL) of distilled water and 100 mM of hydrogen peroxide (1%, v/v) were added. To initialize the reaction, 10 mL of this solution were added to a glass bottle containing 3 mg of Cu hybrid and stirred gently at room temperature on an orbital shaker (320 rpm). At different times samples (100 µL) were taken and the reaction was followed by HPLC. Samples were first centrifuged at 8000 rpm for 5 min and then 50 µL were diluted 20 times in bi-distilled water before injection. HPLC column was C8 kromasil 150 × 4.6 mm AV-2059. HPLC conditions were: an isocratic mixture of 15% acetonitrile and 85% bi-distilled water, UV detection at 270 nm, and a flow rate of 0.4 mL/min. Under these conditions, retention times of pAP and H_2O_2 were 8.5 min, and 4.2 min respectively. The possible adsorption of substrate to the catalyst was first tested and without the presence of hydrogen peroxide no reaction was observed and the full area of the substrate was unaltered in the HPLC analysis.

In the case of **Cu-CALB**, reaction was repeated in the presence of 0.1 mmol of TEMPO (48 mg of polymer-bound TEMPO).

2.9 Stabilization of the Cu nanozymes

The stability of different Enzyme/CuNPs hybrids was evaluated by incubating for 1 h them at different T, the presence of co-solvent or additives (1 mM of known tyrosinase inhibitors). Then, the tyrosinase-like activity of hybrids and enzymatic activity of

tyrosinase from mushroom (TYR) was used for monitoring the stability, considering the activity at 25ºC in each case as 100%. The activity was determined using the DOPA assay described above. In the case of the presence of tyrosinase inhibitors, the activity evaluation was performed at 25ºC in aqueous media.

2.10 Cell Cultures

HT29 (human colon adenocarcinoma) and HeLa (human cervix epithelioid carcinoma) cells were obtained from ATCC and maintained in Dulbecco's Modified Eagle's Medium (DMEM) (PAN-Biotech GmbH, Germany) supplemented with 10% FBS (Fetal Bovine Serum), 1% P/S (Penicillin/Streptomycin) and 1% NEAAs (Non-Essential Amino Acids) at 37 °C with 5% CO_2.

2.11 Cell Viability Assays

Cellular cytotoxicity was assessed in two cell lines: HT29 and HeLa cells. Cells were plated in 96-well plates (8,000 cells/90µl/well in HeLa cells; 9,000 cells/90µl/well in HT29 cells) with supplemented DMEM without phenol red. Twenty-four hours later, 10 µl of several serial dilutions of the compounds were added to the cells (the solutions were prepared at 10X and the maximum concentration of compounds added to cells was that one in which there were 5% of H_2O in each solution). The cells were in presence of the compounds during 24 hours and after this period the cytotoxicity were checked by a MTT-based assay. MTT reagent (3-(4,5-Dimethylthiazol-2-yl)-2,5-diphenyl tetrazolium bromide) (Sigma Corp., St Louis, MO, USA) was prepared by dissolving 5 mg in 1 ml PBS. The stock solution was protected from light and stored at 4°C. To determine cytotoxicity, media was removed from wells and 50 µl of the working MTT solution (1mg/ml in DMEM without phenol red) was added to each well and incubated at 37°C

for 3 h in a humidified, 5% CO_2 atmosphere. After that, the media was carefully removed and the cells were solubilized into 100 µl of isopropanol (Scharlab, S.L., Barcelona, Spain). After 15 min shaking cautiously and protected from light, the absorbance was recorded at 570 nm (reference wavelength: 650 nm) using the Synergy HT (BioTek) plate reader. Each experiment was performed in quadruplicate, repeated at least two times, and normalized regarding untreated cell viability.

3. Results and discussion

3.1 Synthesis and characterization of Enzyme/CuNPs hybrids

The preparation of copper nanoparticles hybrids as novel nanozymes was attempted. Here, different enzymes –which involved different conformational structures, dimeric or multimeric complexes or even introducing post-translational modifications– were used in the preparation of enzyme/CuNPs hybrids. In all cases, protein amount of 0.27-0.3 mg/ml dissolved in phosphate buffer pH 7 were incubated with $CuSO_4$ (10 mg/ml) for 16 h. A solid obtained after centrifugation indicates the final process of the Cu hybrids synthesis. The strategy was performed directly in aqueous solution at room temperature using the following enzymes; three different lipases, lipase from *Candida antarctica B* (CALB) (33 kDa), lipase from *(Geo)Bacillus thermocatenulatus* (BTL) (43 kDa) and lipase from *Thermomyces lanuginosus* (TLL) (33 kDa, dimer) and a catalase produced by a genetically modified strain of the fungus *Aspergillus niger* (CAT) (80 kDa, tetramer).

The final step before to get the enzyme/CuNPs hybrids consisted in the lyophilisation of a frozen suspension of the solid. At this term we could obtain at multimilligram scale a set of different Cu hybrids called as **Cu-CALB**, **Cu-TLL**, **Cu-BTL** or **Cu-CAT** respectively.

Wide-angle X-ray diffraction (XRD) analyses revealed a similar XRD pattern for all of enzyme/CuNPs hybrids, displaying characteristic peaks of $Cu_3(PO_4)_2$ (matched well with JCPDS card no. 00-022-0548 and some reports[39-40]) as unique copper species (Fig S1). Transmission Electronic Microscopy (TEM) revealed the formation of small size crystalline nanoparticles on the protein network in the Cu hybrids (Fig.2, Figs. S2-S5). However, the homogeneous nanoparticles distribution and specially the nanoparticles size was different depending on the enzyme used as scaffold. Cu(II) nanoparticles around 3 to 10 nm were generated and we could see in some cases a relation between the size increased with the size of the protein. Larger nanoparticles were obtained with TLL (10 nm) (Fig. 2b). The explanation of the size and the less homogeneity of the nanoparticles with this enzyme could be because of the extremely high capacity of this enzyme to aggregation,[41] which has been crystallized in tetrameric or even octameric form, therefore we can consider this case a real enzyme unit as more than 100 kDa. Comparing CALB to CAT, we can see clearly that then size of nanoparticles increased from 3.9 (for CALB, Fig 2a) to around 6 nm because of the protein size (Fig.2).

Thus, in the case of BTL, although is a slight larger protein than CALB, Cu(II) nanoparticles of 6.6 nm were obtained (Fig.2c).

ICP-OES analysis showed that the copper content in the different hybrids was quite similar (34-37%), with the exception of TLL with a Cu content of 44% (Table S1).

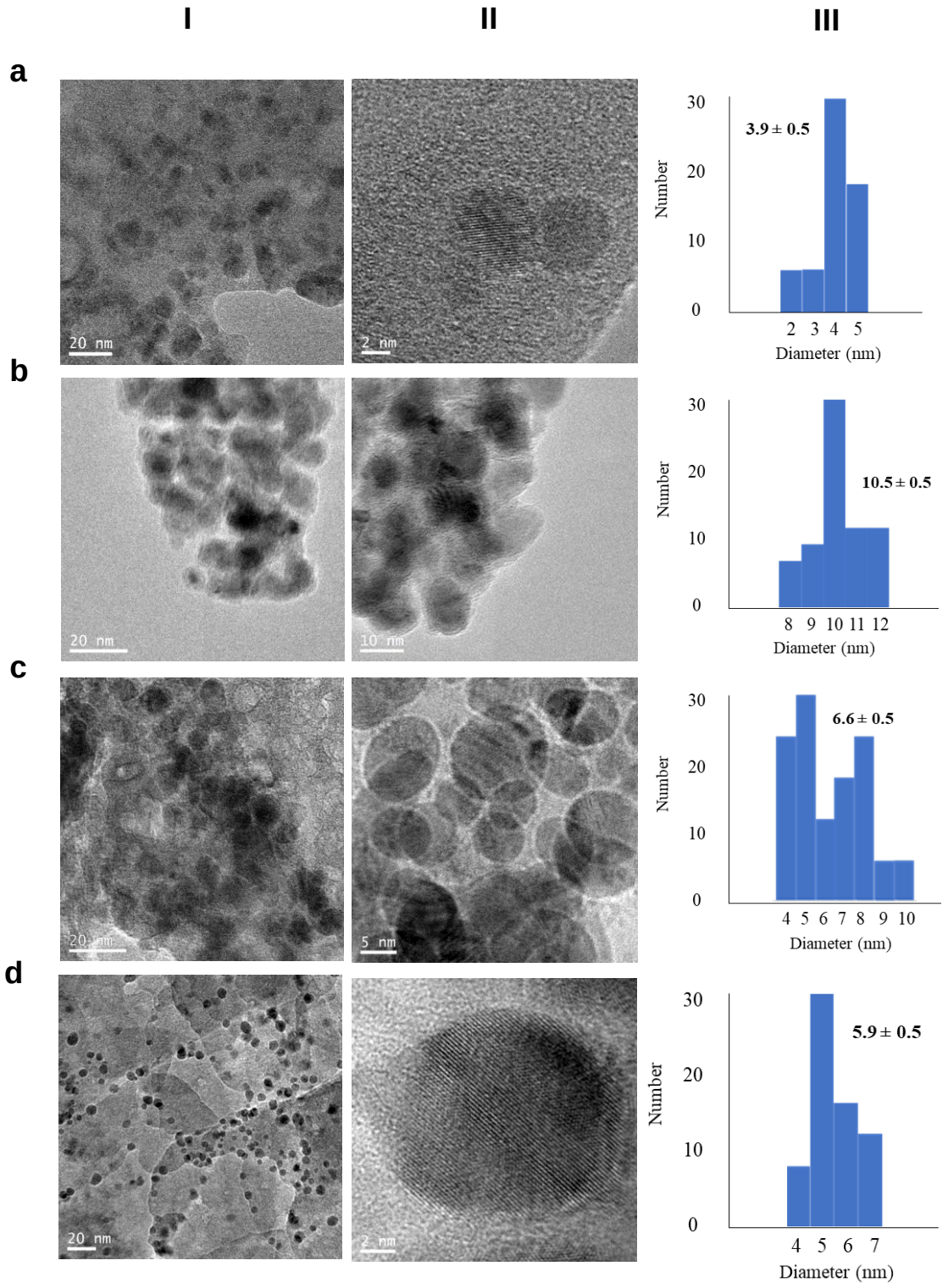

Figure 2. Characterization of different Enzyme/CuNPs hybrids. (a) **Cu-CALB**. (b) **Cu-TLL.** (c) **Cu-BTL. (d) Cu-CAT.** I) Transmission Electronic Microscopy **(**TEM) images; II) High Resolution **(**HR)-TEM images; III) Nanoparticle size distribution.

3.2 Spectroscopic characterization of the Enzyme/CuNPs hybrids.

Experiments of Far circular dichroism (CD) to studying the effect of the modification on the secondary structure of enzymes, and Near CD and fluorescence assays to analysing the effect on the tertiary structure were performed (Fig.3). Far CD spectrum signal obtained was lower in Cu-CALB hybrids in comparison to soluble CALB, but there was still some residual α helix secondary structure (according to the peaks at ~208 and ~222 nm) (Fig. 3a). Same behaviour was found for the rest of enzyme/CuNPs hybrids (Fig.3b). Shape and amount of residual signal were similar in all Cu hybrids.

CALB Near CD spectrum signal was low and in case of enzyme/CuNPs hybrids was lower (or even negligible in some cases) (Fig.3c and 3d) and this meant that tertiary structure was altered upon Cu-enzyme derivative formation.

The fluorescence of protein tryptophan's emission at 345 nm (upon 275 nm excitation) have demonstrated to be quenched by copper and shifted to higher wavelengths (around 400 nm).[42]A similar behaviour was found in these enzyme/CuNPs hybrids. Tryptophan fluorescence signal of CALB soluble enzyme exhibited a peak at 320 nm (upon 280 nm excitation) which was not present in **Cu-CALB** hybrids (Fig. 3e) neither in the rest of enzyme/CuNPs hybrids (Fig.3f). However, we observed a clear signal at 385 nm in the fluorescence spectra of all six Cu hybrids (Fig. 3f), which is characteristic of a Cu^{2+}-enzyme complex formation.[43]

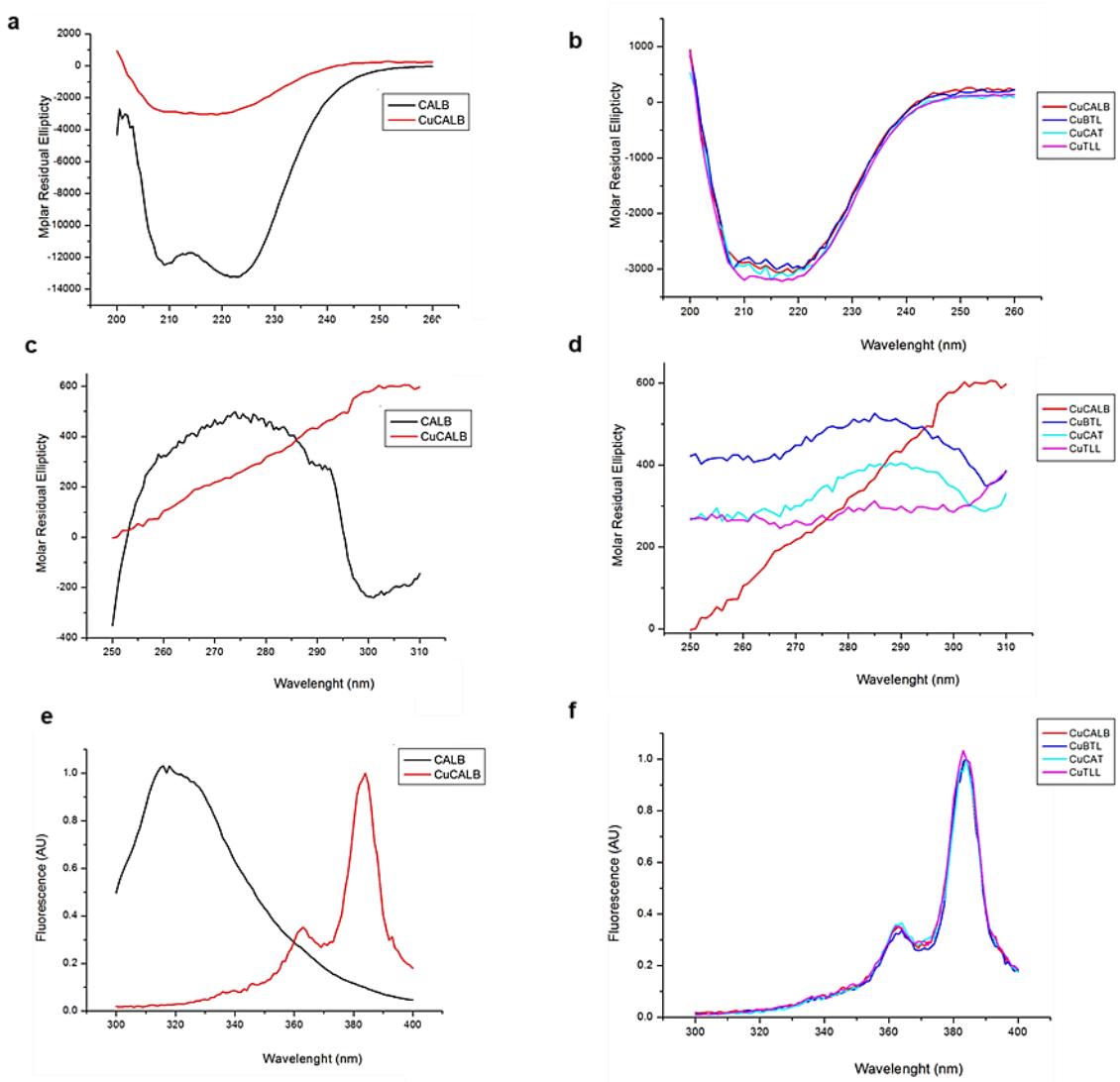

Figure 3. Spectroscopy characterization (CD and fluorescence) of the different Enzyme/CuNPs hybrids. (a) Far-CD spectra of **Cu-CALB** hybrid compared to soluble CALB. (b) Far-CD spectra of the different Cu hybrids. (c) Near-CD spectra of **Cu-CALB** hybrid compared to soluble CALB. (d) Near-CD spectra of the different Cu hybrids. (e) Fluorescence spectra of **Cu-CALB** hybrid compared to soluble CALB. (f) Fluorescence spectra of the different Cu hybrids. Fluorescence measurements were performed using an excitation wavelength of 280 nm, with excitation and emission bandwidths of 5 nm.

3.3 Tyrosinase mimicking activity of different Enzyme/CuNPs hybrids.

Copper tyrosinases (Tyr) represent a very important class of oxidases with key role in catalytic biological systems.[26-27] However, high difficulty to obtain high stable proteins with high level of expression makes them an excellent example of type enzyme where artificial metalloenzyme can be a challenge. These enzymes can catalyze: (i) the *o*-hydroxylation of monophenols to *o*-diphenols as well as (ii) the oxidation of *o*-diphenols

to produce o-quinones. In contrast, and by definition, catechol oxidase can only catalyze the oxidation of o-diphenols to their corresponding o-quinones. Here, catechol oxidase-like activity of the different enzyme/CuNPs hybrids was evaluated using L-3,4-dihydroxyphenylalanine (DOPA) and its derivative L-DOPA methyl ester (DOPAME) as substrate. Both of these compounds do not absorb in the visible region; however, the oxidation produces a chromogenic product (dopachrome) which is brown in color and absorbs at 475 nm (Fig. 4).

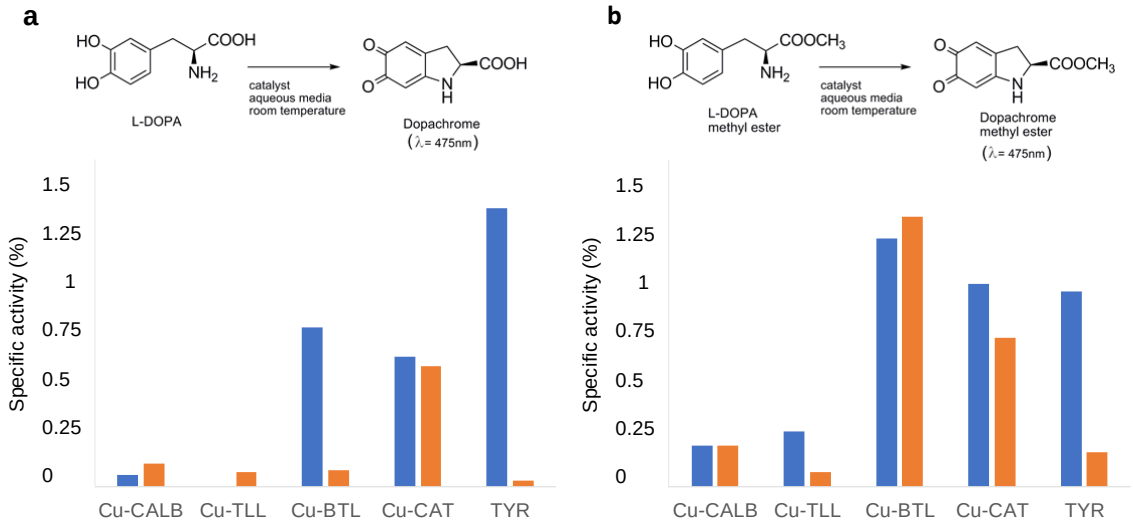

Figure 4. Tyrosinase-like activity of different Enzyme/CuNPs hybrids. (a) Oxidation of L-DOPA at different conditions expressed in values of specific activity (U/mg_{cu} for hybrids or mg_{prot} for TYR). (b) Oxidation of L-DOPA methyl ester at different conditions expressed in values of specific activity (U/mg). Distilled water (blue column), pH 4 (orange column). The activity value of TYR is $x10^2$.

In distilled water and using DOPA as substrate, **Cu-BTL** showed the highest catechol oxidase activity, almost 1 U/mg, between all the enzyme/Cu hybrids (Fig 4a). However, using the other two Cu hybrids synthesized using lipases, little (**Cu-CALB**) or even no catechol-like activity (**Cu-TLL**) was observed.

However, the evaluation of the activity at acidic conditions (pH 4) give a tremendous difference, especially for the hybrid synthesized using BTL which exhibited 10 times less

catechol-like activity, being at these conditions quite similar for all the lipases. This result was also detected when the catechol activity of mushroom from *Agaricus bisporus* tyrosinase (TYR) was evaluated. This is a well-known enzyme which normally is used as a model of the human tyrosinase because both have a very high structural homology.[44]

However, when catalase was used as enzyme for Cu hybrid formation, the **Cu-CAT** hybrid showed only slight lower activity than **Cu-BTL** at pH around 6-7, although was stable to the pH change, with hardly any variation in activity, being the most active Cu hybrid (more than 5 times respect to all others) at pH 4 (Fig 4a). This is interesting because at these conditions, the catechol activity of this **Cu-CAT** hybrid is only slight lower than the natural TYR (which showed specific activity of 3 U/mg) (Fig. 4a, Table S2).

In all hybrids, the catechol-like activity is provided exclusively by the CuNPs synthesized in the hybrids, and no catechol activity was found with enzymes used as scaffold (Table S2).

The catechol-like activity of the Cu hybrids using DOPAME as substrate demonstrated the importance effect of the blocking the negative charge of the carboxylic group in the substrate. Almost in all cases, the activity of the hybrids increased using DOPAME respect to the activity against DOPA. However, TYR showed a decrease (almost 2-fold in distilled water) in the enzymatic activity when the DOPA derivative was used (Fig 4b, Table S3). As occur with L-DOPA, the different enzymes used in the synthesis of Cu hybrid did not show activity against DOPAME (Table S3).

In distilled water as solvent, the **Cu-BTL** hybrid showed the highest activity between all hybrids (Fig.4b). **Cu-TLL** was active against DOPAME (0.275 U/mg), in similar values than **Cu-CALB**.

The effect of pH concerning to the structure of the protein into activity value, was clearly shown when the hybrids activity was evaluated at pH 4 (Fig 4b). Using DOPAME, **Cu-BTL** and **Cu-CALB** hybrids maintained the same catechol activity than that in distilled water, although the decrease in the activity value was found for **Cu-TLL**, in which clearly the pH conditions are more critical for the Cu-sites environment. TYR showed around 5 times higher activity at acidic conditions (Fig 4b) against this substrate compared to DOPA (Fig 4a).

These results could be explained considering the size of the nanoparticles, for example the synthesis using BTL or CAT as enzymes produced hybrids containing smaller CuNPs than TLL.

Nevertheless, the structural microenvironment created by the particular enzyme, coordination with copper and amino acid surrounding area, is a key parameter affecting activity of Cu active sites. Indeed, the isoelectric point (pI) of the enzyme used as scaffold had also an important influence in the final catalytic capacity of the Cu sites independently to the nanoparticle size in each case. In this way, it could be detected a higher catechol activity in DOPA assay when enzyme used as scaffold showed a higher pI, enzymes present a pI of 7.2 for BTL, 6.8 for CAT, 6.0 for CALB and 4.4 for TLL (Figure 4). In this term, at acidic pH, hybrid synthesized using BTL showed the strongest effect on the activity, whereas Cu hybrids created by using CALB or TLL even suffered an increase of efficiency compared to the former conditions. When the substrate presented the carboxylic group blocked (DOPAME), only slight changes were observed in almost all hybrids, being the best the BTL one. Considering the pH effect, in the case of **Cu-CALB** hybrid, an increase of eight times the catechol activity was observed when the DOPAME reaction was performed at pH 7(Fig S6).

All these results demonstrated the key role of the protein environment on the final Cu activity.

3.4 Catalase-like activity

Catalase enzyme is essential for the elimination of the excess of cytoplasmic hydrogen peroxides by converting them to water and molecular oxygen. However, most of the activity described in the literature for other Cu hybrid materials consists in peroxidase-like activity.[45]

Initially, we tested the peroxidase-like activity of these Cu hybrids using the glucose assay and no activity was found for these Cu hybrids (Fig S7). However, the Cu hybrids degraded the hydrogen peroxide to oxygen in distilled water at room temperature (Fig.5). The Cu hybrids prepared using lipases showed similar specific activities, slightly higher for **Cu-BTL** (2.48 U/mg).

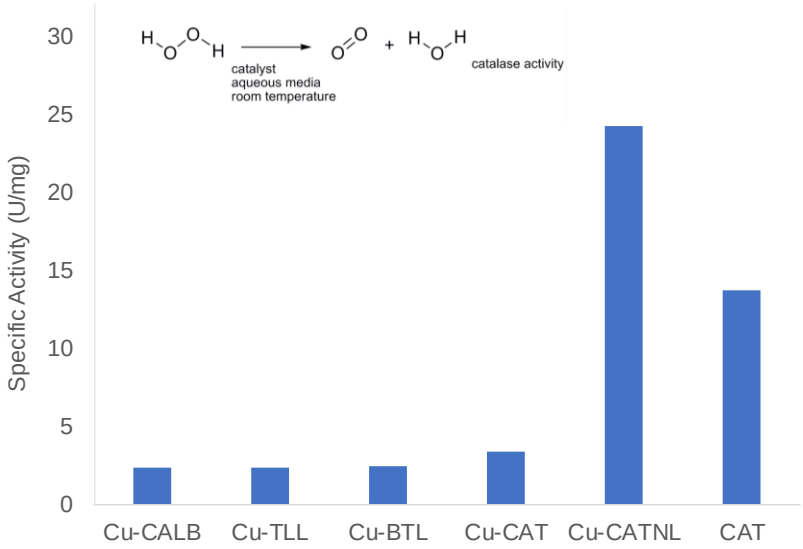

Figure 5. Catalase-like activity of different Enzyme/CuNPs hybrids.

However, the degradation of hydrogen peroxide is the natural catalytic reaction of catalase, which at these conditions showed a specific activity of 13 U/mg. Thus, the

preparation of a Cu hybrid using this enzyme as scaffold could allow to synthesize a nanozyme with a double activity, a synergy between the natural and the metallic ones.

However, the **Cu-CAT** hybrid showed only a slightly better activity then the previous hybrids, around 3.38 U/mg, which correspond to around 25% of initial catalase activity of the soluble native enzyme (Fig 5).

One of the explanations could be that it is demonstrated that catalase loss more than 80% activity after lyophilization,[46] the last step in the preparation of this hybrid.

Therefore, in order to avoid this drawback, the synthesis of the Cu hybrid using catalase as enzyme scaffold was performed following the previous protocol without the lyophilization step, just simply washed and store the solid re-suspended in distilled water.

The characterization of this hybrid without freezing (Fig. S8), showed that Cu species were conserved as copper phosphate (XRD analysis), with the formation of homogeneous spherical nanoparticles of 8 nm of size diameter (TEM analysis), slightly higher than generated with the freezing step (Fig 2). ICP-OES analysis determined that the amount of copper was also conserved the same.

This **Cu-CAT-NL** hybrid showed much better catalase activity, 8 times respect to that of the lyophilized version (**Cu-CAT**), showing a clear synergy between enzyme and CuNPs in catalyse activity, with double activity compare to free CAT.

The maintaining of the enzyme structure seems to be again important effect on the CuNPs besides to the directly intrinsic enzymatic activity.

3.5 Dual-activity of Cu-enzyme hybrids.

Studies have been demonstrated that the presence of oxygen in the media enhanced the catalytic efficiency of tyrosinase or catecholase in the DOPA reaction.

Considering the previous results of **Cu-CAT-NL** in catalase activity in the production of free oxygen in solution from hydrogen peroxide, and their catecholase activity against L-DOPA, slightly lower than the observed for **Cu-CAT**, a tandem system combining L-DOPA and hydrogen peroxide, where oxygen *in situ* could be performed by the natural enzyme (catalase) for enhancement of the catechol activity of the CuNPs sites was evaluated (Fig. 6).

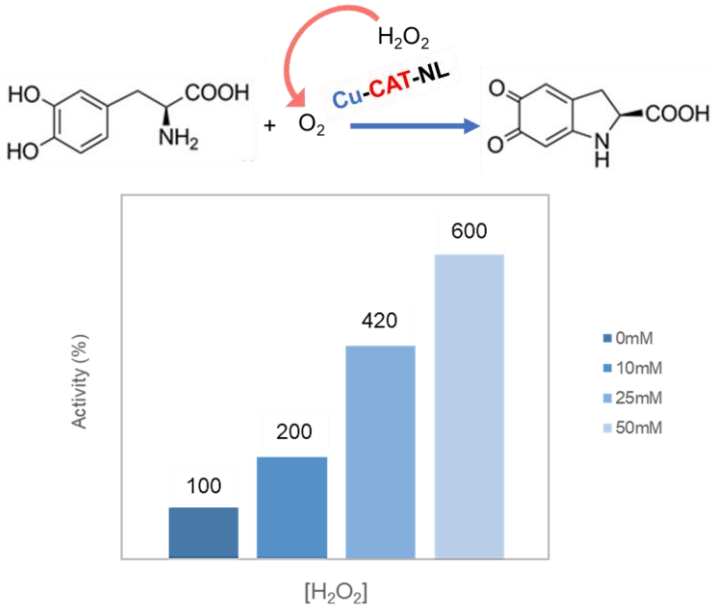

Figure 6. Synergy effect (enzyme plus metal) in the cathecol-like activity of Cu-CAT-NL. The specific activity of this hybrid in absence of hydrogen peroxide was considered as 100% activity percentage.

Thus, the **Cu-CAT-NL** hybrid was evaluated in the oxidation of L-DOPA in the presence of different concentrations of hydrogen peroxide (Fig 6).

The results showed how effectively the catecholase activity of the biohybrid increased importantly, up to 6 times, when there was hydrogen peroxide (50 mM) in the medium, due to the synergistic reaction with catalase (enzyme like scaffold), which increases the presence of oxygen in the medium by degradation of hydrogen peroxide. Lower amounts of hydrogen peroxide also improved the catechol activity of the hybrid but to a lesser

extent, showing how the cascade system gave rise to an increase in an initially impaired enzymatic activity due to a combined effect between enzymatic and metallic activity of the biohybrid.

3.6 Fenton catalyst

After these excellent results in modulating tyrosinase and catalase activity, we try to evaluate the effect of the enzyme structure on the fenton catalysis of the different hybrids. The selective hydroxylation of p-aminophenol to benzoquinone using hydrogen peroxide as green oxidant was used (Fig 7). Fenton process was observed with these Cu Hybrids. A clear tendency was observed in the case of using lipases as enzyme scaffold, where higher conversion the smaller size cu nanoparticles. However, the best result was found using CAT as enzyme, with almost 90% conversion in 7 min, which indicate the influence of the enzyme structure together the nanoparticle size.

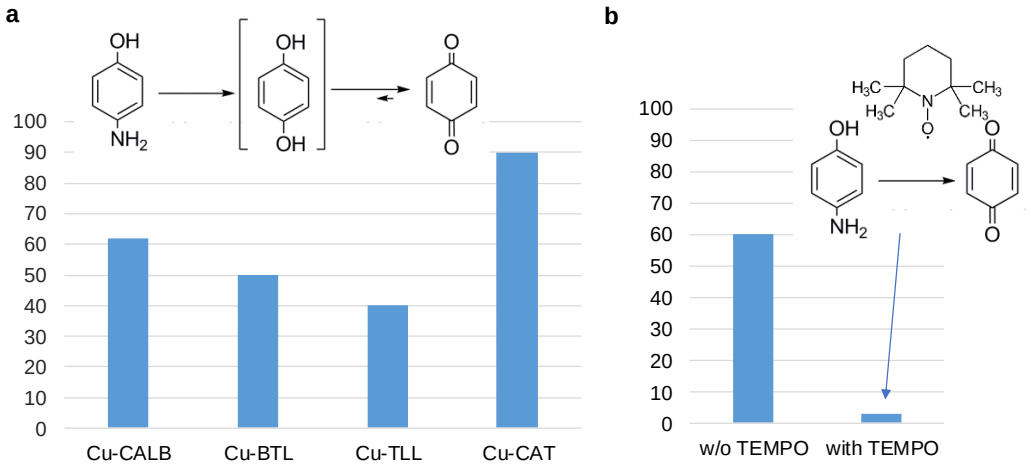

Figure 7. Fenton-catalysis in the hydroxylation reaction of p-aminophenol to benzoquinone. (a) Conversion of different Cu hybrids after 8 min reaction. Conditions: 100mg/L of pAP in 10 mL of distilled water, 1%, v/v of H_2O_2 and 3 mg of Cu hybrid at room temperature. (b) Reaction catalysed by **Cu-CALB** with or without TEMPO.

Furthermore, in order to demonstrate the Fenton process mechanism of the reaction, with radical OH· formation, the reaction was also performed in the presence of TEMPO using **Cu-CALB** as catalyst (Fig 7b). At these conditions, only 3% conversion was observed

after 7 min (60% without adding TEMPO) with a clear decrease in the reaction process in the reaction profile.

3.7 Assessing cell metabolic activity of the Enzyme/CuNPs hybrids on cancer cells

One of the emerging applications of nanozymes is going to focus for *in vitro* nanocatalytic therapeutic efficiency.

In this term, *in vitro* cytotoxic activity of the Cu hybrids has been evaluated in two different cancer cell lines, HeLa (human cervical cancer) and HT29 (human colon cancer cells). Different concentrations of the Cu hybrids were used in the assay after 24 h incubation. The cell metabolic activity was determined by using the colorimetric MTT (3-(4,5-dimethylthiazol-2-yl) -2,5- diphenyltetrazolium bromide or methyl thiazole tetrazolium) bromide) assay (Fig 8).

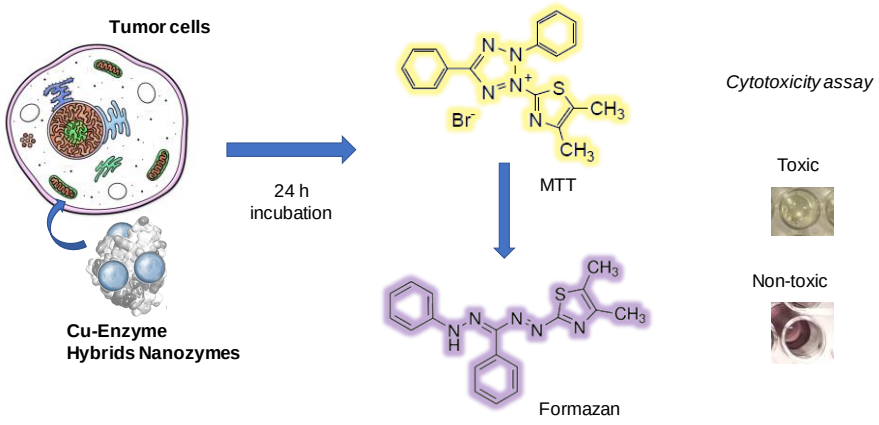

Figure 8. Schematic of the MTT assay

The essence of this assay is based on the metabolic reduction of (MTT), which is carried out by the enzyme Mitochondrial succinate dehydrogenase from metabolically active mitochondria cells. This enzyme transforms MTT from a yellow hydrophilic soluble compound to a blue hydrophobic insoluble compound (formazan) (Fig 8) by cleavage of the tetrazolium ring by dehydrogenase enzymes. Consequently, that transformation enables the mitochondrial function of the treated cells to be determined. The product of

the reaction, the formazan, is retained in the cells and can be released by the solution thereof. The ability of cells to reduce MTT is an indicator of the integrity of mitochondria.

Viability according to Cu content in hybrids is represented in Fig 9**.** Differences in cell viability depending on the Cu hybrids used can be found and also different effect depending on the cancer cell lines, showing higher cytotoxicity against HeLa cells (Fig 9). **Cu-CALB** and **Cu-TLL** showed the best cytotoxicity at lower concentration (0.1 lower concentrations.

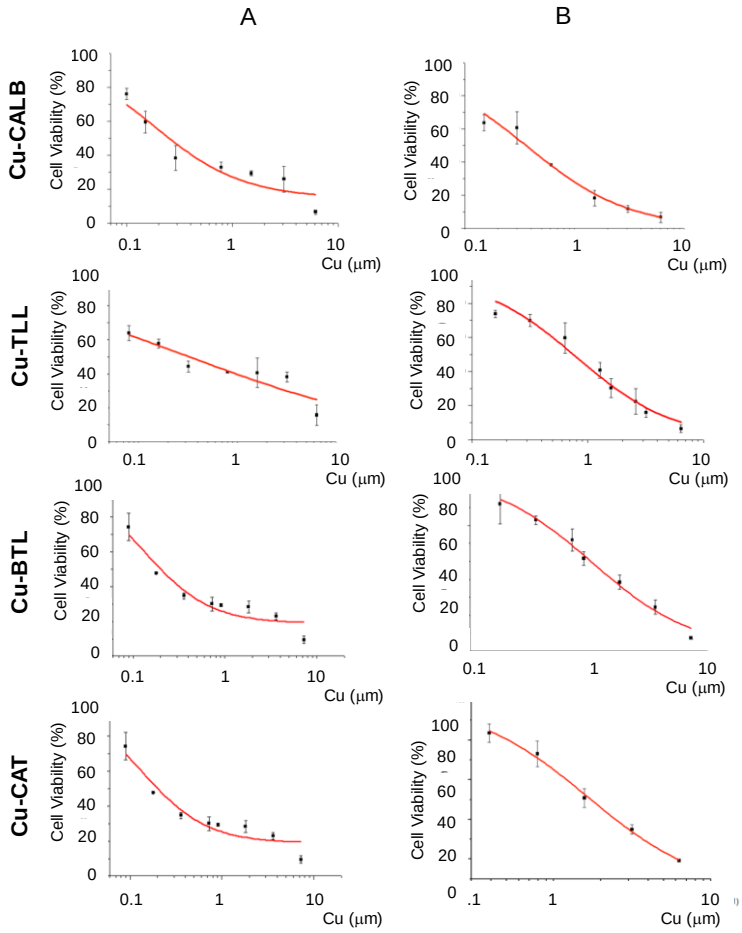

Figure 9.Curve cell viability in cancer cells calculated in µM concentration of Cu of Cu-hybrids. A. HeLa cells; B. HT29 cells.

The concentration of copper in which 50% of initial activity is reached (LC50) (Table 1) was determined from the fitting of these curves in Fig 9.

HeLa cells seemed to be more sensitive to Cu than HT29 cells, up to ten times in case of **Cu-BTL** hybrid (0.13 and 1.05 μM of Cu respectively), which showed the lowest LC50 values in HeLa cells (Table 1). In the case of **Cu-CAL-B**, this showed the lowest LC50 values (0.37μM of Cu) in HT29 cell lines also being one of the best in cytotoxicity against HeLa cells. **Cu-CAT-NL** exhibited the highest LC50 values in HeLa and HT29 (1.25 and 1.65 μM of Cu respectively). **Cu-TLL** (0.33 and 0.8 μM of Cu) is in between the highest and lowest values. The different enzymes used for preparing the hybrid were tested and no cytotoxicity was found (Fig S9).

Thus, **Cu-CALB** hybrid, which present the smallest size in Cu nanoparticles, seemed to be the enzyme-like derivative with the highest cytotoxic activity in the tested cell cultures. It has been reported that Cu can generate reactive oxygen species (ROS) in the cell and ROS increment causes DNA damage.[47-48] According to the results of this work, our Cu-enzyme hybrids exhibited antitumor properties, as other Cu compounds previously described in literature probably based on the oxidative enzyme-mimic capacity (such as xanthine oxidase or monoamine oxidases-like activity) of the Cu nanoparticles on them.

Table 1. LC50 (μM) of the different Cu-enzyme hybrids on HeLa and HT29 cell lines.

Cu-Hybrid	HeLa LC50 Cu (μM)	HT29 LC50 Cu (μM)
Cu-CALB	0.18	0.37
Cu-BTL	0.13	1.05
Cu-TLL	0.33	0.8
Cu-CAT	1.25	1.65

3.8 Protein Structural effect of the enzymes as scaffold in the formation of the enzyme/CuNPs hybrids.

The use of an enzyme in the nanozyme synthesis has a key role in the stabilization and the formation of homogenously distributed copper nanoparticles and their stabilization on the protein network.

Indeed, the formation of hybrid copper nanoparticles first undergoes by a rapid coordination between particular amino acid residues of the enzyme with the copper ions, generating enzyme–Cu(II) intermediates (Fig. 1). It is well described that copper ions have very good coordination capacity, especially with carboxylic groups (Asp, Glu) and also with amino groups, mainly those containing histidine residues. Interaction with cysteine residues may also be possible.

However, the three-dimensional environmental area around these coordinated groups, which can be different depending on the enzyme, seems to awarding a critical role. In this case we have seen that employing different enzymes, the same Cu species were formed.

Therefore, bioinformatics analyses were performed to evaluate the structural environmental effect of the enzymes into the enzyme-like activity of the CuNPs sites in the different hybrids (Fig 10, Fig S10-11).

In particular, in the case of catechol-like activity, Cu hybrid synthesized using BTL showed the highest enzymatic activity in all cases, being also affected by the pH on the activity specially using L-DOPA (Fig 4).

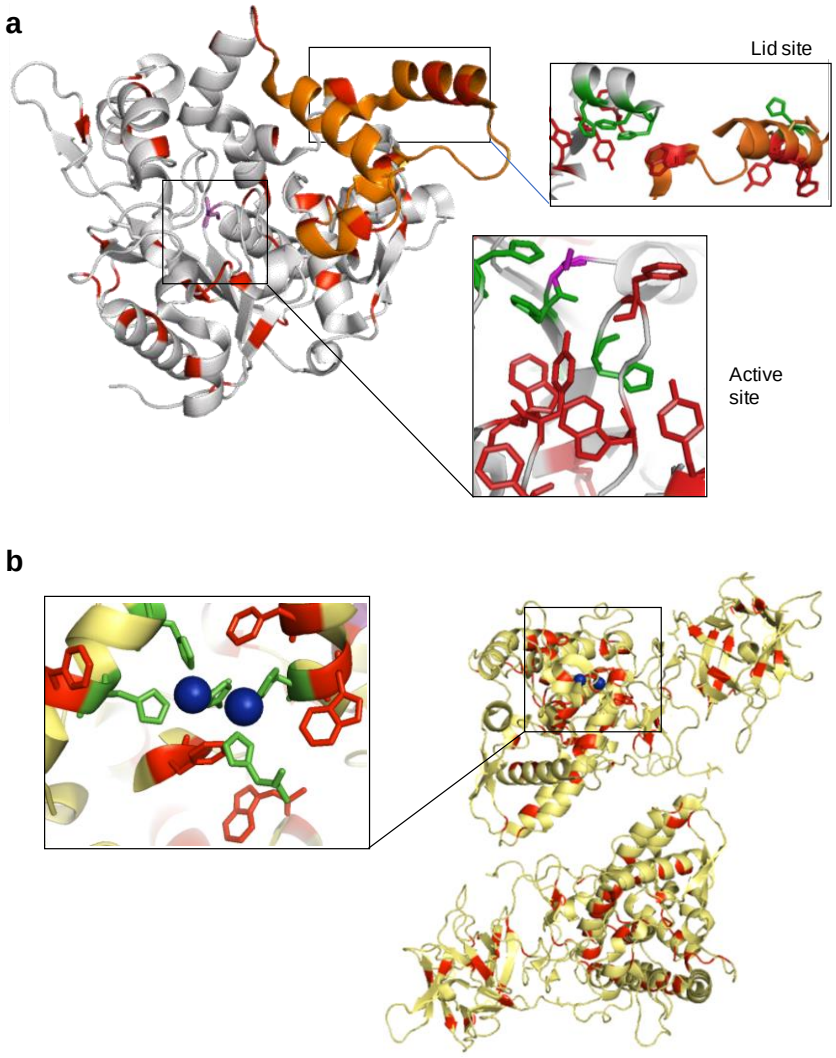

Figure 10. Crystal structure of *B. thermocatenulatus* lipase and mushroom Tyrosinase. (a) Cartoon of the crystallized *B. thermocatenulatus* lipase (BTL) with aromatic aminoacids (Trp, Tyr, Phe) in red, histidine residues in green, the catalytic serine in magenta and the oligopeptide lids in orange. (b) Cartoon of crystallized mushroom tyrosinase (TYR) with aromatic aminoacids (Trp, Tyr, Phe) in red, histidine residues in green and Cu atoms in blue. The protein structures were obtained from the Protein Data Bank (PDB code: 2w22 (BTL) and 2y9w TYR) and the picture were created using Pymol v. 0.99.

This is a specific lipase, which present an extremely hydrophobic area surrounding the active site, where also is located an area containing His residues (imidazole groups) where Cu can be coordinated (Fig 10a). Metal-binding sites in proteins are commonly formed from loops, because these regions are reasonably tolerant to sequence modifications outside of coordinating residues.

Furthermore this lipase present another interesting area, near to one of the two lids involved in the catalytic mechanism of the enzyme,[49] where we can found a perfect tri-histidine pocket (Fig 10a) as quite similar as exist in the natural tyrosinase (Fig 10b)[44] Both His pockets are surrounded by different aromatic aminoacid residues (e.g. Trp, Phe or Tyr), which are important in the substrate stabilizing the catechol group near to the Cu binding position on the protein for permitting the catalytic transformation, as occur in the natural enzymes. It has been demonstrated that lipase mechanism has strong influence on the pH, specially this thermoalkalophilic one,[49] so results achieved of loss of catechol-like activity in acidic pH or different effect using DOPAME as substrate clearly demonstrate that the typical structural form of this lipase have an influence in the final CuNPs site catalysis.

Cu-hybrids synthesized using catalase, involved the use of a multimeric enzyme, with four identical subunits of 80 kDa. Each subunit presents 20 histidine residues, for successful coordination of Cu ions and huge number of aromatic amino acid residues (Fig S10). This could indicate, although unfortunately the structure of catalase from *A. Niger* is still not solved, that structural environment (similar than in BTL case) could be involved in the final good activity of CuNPs sites.

An opposite result was obtained with TLL, even no catechol activity was found in some condition. This lipase has a huge trend to form aggregates –even of 8 molecules- make it in aqueous solution as a complex enzyme.[41]This could be the reason why TLL produced the larger nanoparticles size compared with CALB, lipase with the same molecular weight in monomeric form[50] (Fig S11). This property has influence on natural activity of the enzyme and clearly is also a handicap for the catechol-like activity.

3.9 Stability of the enzyme/CuNPs Nanozymes

Another important property of the enzyme is the stability. In particular, tyrosinase has been detected as not so stable after biological conditions. In this point, the stability of the most active Cu hybrids, in comparison with TYR, was evaluated at different T and in the presence of co-solvent (Fig 11). TYR was rapidly inactivated at 37ºC, and conserving only 38% of the initial activity after 1 h incubation, using DOPA as substrate (Fig 11a). However, the stability of TYR was better using DOPAME as substrate conserving more than 50% activity after 1h incubation at 37ºC (Fig11b). The stability of this enzyme in the presence of 40% (v/v) acetonitrile at room temperature was also low, conserving around 45% initial activity value after 1 h incubation.

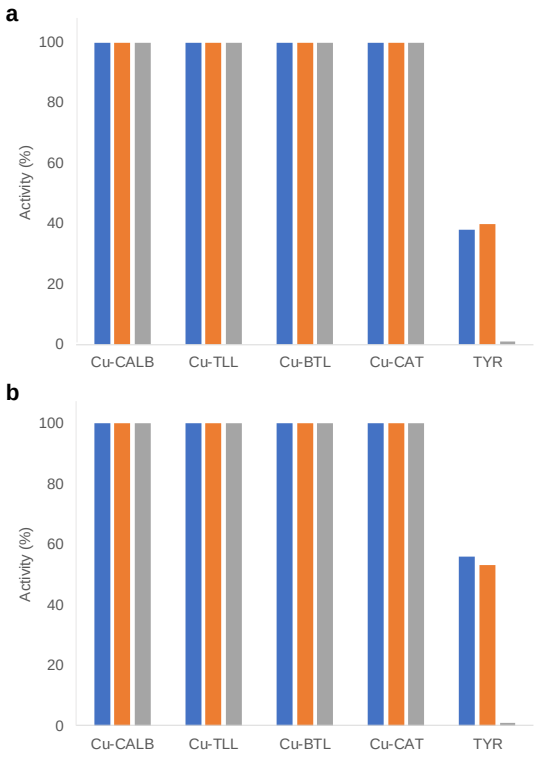

Figure 11. **Stability of different Enzyme/CuNPs hybrids *vs* tyrosinase (TYR) in catechol-like activity.** A) Oxidation reaction of L-DOPA. B) Oxidation reaction of L-DOPAME. 37ºC (blue column), 40% (v/v) acetonitrile (orange column), 37ºC and 40% (v/v) acetonitrile (grey column).

The combination of both elements, T and co-solvent caused a complete inactivation of the enzyme after 1 h incubation (Fig 11).

The different Cu hybrids synthesized conserved 100% of their catechol-like activity after 1 h incubation of any of these conditions (Fig 11), demonstrating that these nanozymes could represent an alternative to sensitive enzymes in many processes. These enzymes used as scaffold were stable at these experimental conditions (data not shown), which could be important in term of maintaining the three-dimensional structure which also was observed in the circular dichroism and fluorescence experiments (Fig 3).

In term of stability, one of the disadvantages of enzymes is the possible inhibition by substrates. In particular, mushroom tyrosinase (TYR) activity has been demonstrated to be inhibiting by different conjugated or aromatic compounds. Here, four of these known substrates[51](L-ascorbic acid, *trans*-cinnamaldehyde, benzaldehyde or 4-metoxy benzaldehyde) have been added in the catechol assay and activity of the Cu hybrids have been measured (Fig 12).

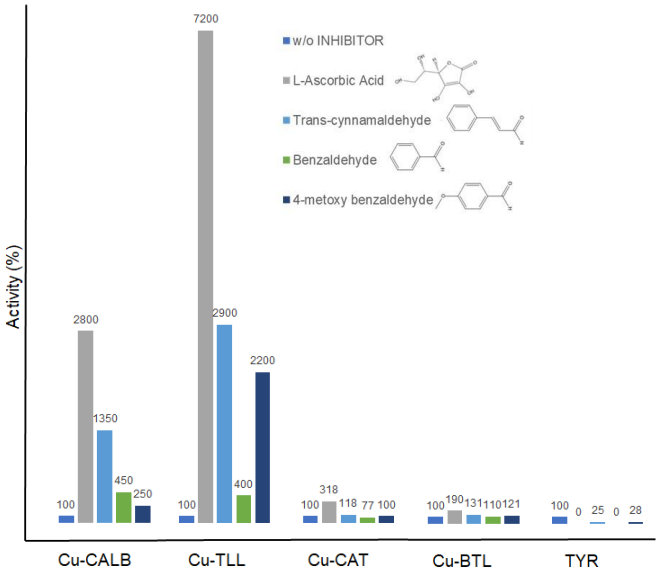

Figure 12. Tyrosinase activity of different Cu-enzyme nanohybrids *vs* TYR in the presence of different tyrosinase-inhibitors. L-DOPA in distilled water assay was used. Conditions: 1 mM L-DOPA in 2 mL of distilled water at r.t. The inhibitors were added at 1mM.

TYR activity was rapidly inhibited in the presence of these substrates, only conserving some activity (25% of initial activity) against Trans-cynnamaldehyde and 4-methoxybenzaldehyde (Fig 7).

However, Enzyme/CuNPs hybrids did not suffer any inhibition, indeed in some cases an hyperactivation was observed in the presence of these molecules (Fig 12). Very surprising could be the increase of catechol-like activity of hybrids synthesized using CALB and especially using TLL. In particular, Cu-Hybrids containing TLL improved 72-fold its previous catechol activity in the presence of ascorbic acid, while hybrid with CALB did it 28 times (Fig. 12). However, this effect could be explain considering the reported increase in hydrolytic activity of CALB in the presence of aromatic or conjugated compounds[52] or in the case of TLL, which activity was increased more than 600 times in the presence of small amount of CTAB (cationic detergent).[53] Therefore, these results seem to show that the protein structure have an important influence changing the catalytic capacity of the Cu active sites on it.

Conclusion

Enzyme/CuNPs hybrids with a controlled nanoparticle sizes and environment have been successfully synthesized by using different enzymes. The difference between enzymes, where we can use three different lipases with a particular catalytic mechanism and the use a supramolecular tetrameric catalase demonstrates the important effect of the structure in the final catalytic properties as nanozymes.

In particular, the oxidase-like catalytic activity of these copper nanozymes was rationally modulated by the enzyme used as scaffold with important ability to mimics a unique enzyme activity.

For example, the tyrosinase-like activity of these Cu hybrids was clearly modulate by the enzymes, and **Cu-BTL** was the one showing very high activity against L-DOPA or L-DOPAME oxidation, demonstrating the role of the enzyme used. Importantly, this nanozyme showed extremely high stability in conditions were natural tyrosinase was completely inactive.

In the catalase-like activity, a synergic activity between the Novozymes catalase and CuNPs created on using this enzyme (**Cu-CAT-NL**) permit to achieve a nanozyme with enhanced activity respect to the natural biocatalyst, being quite critical the preservation of the three-dimensional structure of the enzyme as scaffold for that, non-observed when lyophilization step was used in the Cu hybrid creation (**Cu-CAT**).

Furthermore, a very interesting dual activity was found in order to increase the catechol-like activity of the CuNPs in Cu-CAT-NL. In this case the presence of hydrogen peroxide in the L-DOPA assay allowed to greatly improve this activity for the CuNPs by the enzymatic activity in the hybrid (CAT), which generates *in situ* oxygen in the process. This could be interesting for the design of L-DOPA biosensor for detection of tyrosinase, which have been found at elevated amounts on melanoma cancer cells.

In the generation of radical hydroxyl species, fenton catalyst application of the hybrids demonstrated a clear tendency in lipases as scaffold used where the best result was found when smaller size nanoparticles were obtained. In this reaction **Cu-CAT** was however the most reactive one.

This typical nanozymes activity was evaluated in the cytotoxicity of these hybrids in different human cancer cell lines and **Cu-CALB** —which presents the smallest enzyme with the smallest nanoparticle sizes— showed the best antitumor activity.

Therefore, these results showed that different nanozymes of the same Cu species with a tailor-made enzyme-like activity could have potential therapeutic and diagnostic applications.

ASSOCIATED CONTENT

Supporting Information. Supplementary experimental results and data as follows: TEM figures, XRD pattern, SEM figures, enzymatic-like activity results, MTT assay, protein sequences data, ICP-analyses results (PDF).

AUTHOR INFORMATION

Corresponding Author

Jose M Palomo — Department of Biocatalysis, Institute of Catalysis (CSIC). Marie curie 2, Cantoblanco Campus UAM, 28049, Madrid, Spain; orcid.org/0000-0002-6464-1216. E-mail: josempalomo@icp.csic.es

Authors

Noelia Losada-Garcia —Department of Biocatalysis, Institute of Catalysis (CSIC). Marie curie 2, Cantoblanco Campus UAM, 28049, Madrid, Spain; orcid.org/0000-0003-3940-4208.

Ana Jimenez-Alesanco — Instituto de Biocomputación y Física de Sistemas Complejos, Joint Units IQFR-CSIC-BIFI, and GBsC-CSIC-BIFI, Universidad de Zaragoza, Spain; orcid.org/0000-0003-4726-7821.

Adrian Velazquez-Campoy— Fundación ARAID, Gobierno de Aragón, Zaragoza, Spain; Instituto de Biocomputación y Física de Sistemas Complejos, Joint Units IQFR-CSIC-BIFI, and GBsC-CSIC-BIFI, Universidad de Zaragoza, Spain; Fundación Instituto

de Investigación Sanitaria de Aragón (IIS Aragón), Zaragoza, Spain; Centro de Investigación Biomédica en Red en el Área Temática de Enfermedades Hepáticas y Digestivas (CIBERehd), Madrid, Spain; Departamento de Bioquímica y Biología Molecular y Celular, Universidad de Zaragoza, Zaragoza, Spain; https://orcid.org/0000-0001-5702-4538

Olga Abian — Instituto de Biocomputación y Física de Sistemas Complejos, Joint Units IQFR-CSIC-BIFI, and GBsC-CSIC-BIFI, Universidad de Zaragoza, Spain; Fundación Instituto de Investigación Sanitaria de Aragón (IIS Aragón), Zaragoza, Spain; Centro de Investigación Biomédica en Red en el Área Temática de Enfermedades Hepáticas y Digestivas (CIBERehd), Madrid, Spain; Departamento de Bioquímica y Biología Molecular y Celular, Universidad de Zaragoza, Zaragoza, Spain; Instituto Aragonés de Ciencias de la Salud (IACS), Zaragoza, Spain; https://orcid.org/0000-0001-5664-1729.

ACKNOWLEDGMENTS

This work was supported by the Spanish Government and the Spanish National Research Council (CSIC) (projects PIE 201880E011, 201980E081), Fondo de Investigaciones Sanitarias from Instituto de Salud Carlos III, and European Union (ERDF/ESF,'Investing in your future') (PI15/00663 and PI18/00349 to OA); Spanish Ministry of Economy and Competitiveness (BFU2016-78232-P to A.V.C.); Diputación General de Aragón (Predoctoral Research Contract 2019 to A.J.A., 'Protein Targets and Bioactive Compounds Group' E45_20R to A.V.C., 'Digestive Pathology Group' B25_20R to O.A.) and Centro de Investigación Biomédica en Red en Enfermedades Hepáticas y Digestivas (CIBERehd). We thank Dr. de las Rivas for the preparation of the BTL enzyme and Dr. Martinez from Novozymes for the gift of CALB, TLL and CAT enzymes.

REFERENCES

1. Dong, H.; Fan, Y.; Zhang, W.; Gu, N.; Zhang, Y. Catalytic mechanisms of nanozymes and their applications in biomedicine. *Bioconjug. Chem.* **2019**, *30*, 1273-1296.
2. Singh, S. Nanomaterials Exhibiting Enzyme-Like Properties (Nanozymes): Current Advances and Future Perspectives. *Front Chem.* **2019**,*7*, 46
3. Jiang, D.; Ni, D.; Rosenkrans, Z. T.; Huang, P.; Yan, X.; Cai, W. Nanozyme: new horizons for responsive biomedical applications. *Chem. Soc. Rev.* **2019**, *48*, 3683-3704.
4. Song, W.; Zhao, B.; Wang, C.; Ozaki, Y.; Lu, X. Functional nanomaterials with unique enzyme-like characteristics for sensing applications. *J. Mater. Chem. B.* **2019**, *7*, 850-875.
5. Vong, K.; Eda, S.; Kadota, Y.; Nasibullin, I.; Wakatake, T.; Yokoshima, S.; Shirasu, K.; Tanaka, K. An artificial metalloenzyme biosensor can detect ethylene gas in fruits and Arabidopsis leaves. *Nat. Commun*. **2019,** *10,* 1-15.
6. Qiu, H.; Pu, F.; Ran, X.; Liu, C. Q.; Ren, J. S.; Qu, X. G. Nanozyme as artificial receptor with multiple readouts for pattern recognition. *Anal. Chem.* **2018**, *90*, 11775– 11779
7. Tian, L.; Qi, J. X.; Oderinde, O.; Yao, C.; Song, W.; Wang, Y. H. Planar intercalated copper (II) complex molecule as small molecule enzyme mimic combined with Fe_3O_4 nanozyme for bienzyme synergistic catalysis applied to the microRNA biosensor. *Biosens. Bioelectron.* **2018**, *110*, 110– 117,
8. Popov, A. L.; Popova, N. R.; Tarakina, N. V.; Ivanova, O. S.; Ermakov, A. M.; Ivanov, V. K.; Sukhorukov, G. B. Intracellular delivery of antioxidant

CeO_2 nanoparticles via polyelectrolyte microcapsules. *ACS Biomater. Sci. Eng.* **2018**, *4*, 2453– 2462,

9. Yang, B. W.; Chen, Y.; Shi, J. L. Nanozymes in catalytic cancer theranostics. *Prog. Biochem. Biophys.* **2018**, *45*, 237– 255
10. Wang, Z.; Jia, T.; Sun, Q.; Kuang, Y.; Liu, B.; Xu, M.; Zhu, H.; He, F.; Ga, S.; Yang, P. Construction of Bi/phthalocyanine manganese nanocomposite for trimodal imaging directed photodynamic and photothermal therapy mediated by 808 nm light. *Biomaterials* **2020**, *228*,119569.
11. Dong, S.; Dong, Y.; Jia, T.; Liu, S.; Liu, J.; Yang, D.; He, F.; Gai, S.; Yang, P.; Lin, Y. GSH-Depleted Nanozymes with Hyperthermia-Enhanced Dual Enzyme-Mimic Activities for Tumor Nanocatalytic Therapy. *Adv. Mat*. **2020**, 2002439.
12. Xu, M.; Yang, G.; Bi, H.; Xu, J.; Feng, L.; Yang, D.; Sun, Q.; Gai, S.; He, F.; Dai,Y.; Zhong, C.; Yang, P. Combination of CuS and g-C3N4 QDs on upconversion nanoparticles for targeted photothermal and photodynamic cancer therapy. *Chem. Eng. J*. **2019**, *360*, 866–878.
13. Li, S.; Hou, Y.; Chen, Q.; Zhang, X.; Cao, H.; Huang, Y. Promoting Active Sites in MOF-Derived Homobimetallic Hollow Nanocages as a High-Performance Multifunctional Nanozyme Catalyst for Biosensing and Organic Pollutant Degradation. *ACS Appl. Mater. Interfaces* **2020**, *12*, 2, 2581–2590.
14. Zhao,Y.; Yu Huang, Y.; Wu, J.; Zhan, X.; Xie, Y.; Tang, D.; Cao, H.; Wen Yun, W. Mixed-solvent liquid exfoliated MoS2 NPs as peroxidase mimetics for colorimetric detection of H2O2 and glucose. *RSC Adv.*, **2018**,*8*, 7252-7259.

15. Wu, J. J.; Wang, X. Y.; Wang, Q.; Lou, Z. P.; Li, S. R.; Zhu, Y. Y.; Qin, L.; Wei, H. Nanomaterials with enzyme-like characteristics (nanozymes): next-generation artificial enzymes (II). *Chem. Soc. Rev.* **2019**, *48*, 1004-1076
16. Zhou, Y. B.; Liu, B. W.; Yang, R. H.; Liu, J. W. Filling in the gaps between nanozymes and enzymes: challenges and opportunities. *Bioconjugate Chem.* **2017**, *28*, 2903– 2909,
17. Wei, H.; Wang, E. K. Nanomaterials with enzyme-like characteristics (nanozymes): next-generation artificial enzymes. *Chem. Soc. Rev.* **2013**, *42*, 6060– 6093.
18. Wang, X. Y.; Hu, Y. H.; Wei, H. Nanozymes in bionanotechnology: from sensing to therapeutics and beyond. *Inorg. Chem. Front*. **2016**, *3*, 41– 60
19. Liu, B.; Liu, J. Surface modification of nanozymes. *Nano Res*. **2017**, *10*, 1125–1148.
20. Huo, M.; Wang, L.; Zhang, H.; Zhang, L.; Chen, Y.; Shi, J. Construction of Single-Iron-Atom Nanocatalysts for Highly Efficient Catalytic Antibiotics. *Small* **2019**, *15*, 1901834.
21. Zhao, L.; Cai, J.; Li, Y.; Wei, J.; Duan, C. A host–guest approach to combining enzymatic and artificial catalysis for catalyzing biomimetic monooxygenation. *Nat. Commun*. **2020**, *11*, 1-11.
22. Zhang, W.; Dynes, J. J.; Hu, Y.; Jiang, P.; Ma, S. Porous metal-metalloporphyrin gel as catalytic binding pocket for highly efficient synergistic catalysis. *Nat. Commun*. **2019**, *10*, 1-8.
23. Song, Y.; Feng, X.; Chen, J. S.; Brzezinski, C.; Xu, Z.; Lin, W. Multistep Engineering of Synergistic Catalysts in a Metal–Organic Framework for Tandem C–O Bond Cleavage. *J. Am. Chem. Soc*. **2020**, *142*, 4872-4882.

24. Rosenzweig, A. C.; Sazinsky, M. H. Structural insights into dioxygen-activating copper enzymes. *Curr. Opin. Struc. Biol*. **2006,** *16,* 729-735.
25. Solomon, E. I.; Heppner, D. E.; Johnston, E. M.; Ginsbach, J. W.; Cirera, J.; Qayyum, M.; Kieber-Emmons, M. T.; Kjaergaard, C. H.; Hadt, R.G.; Tian, L. Copper active sites in biology. *Chem. Rev*. **2014,** *114,* 3659-3853.
26. Vaaje-Kolstad, G.; Westereng, B.; Horn, S. J.; Liu, Z.; Zhai, H.; Sorlie, M.; Eijsink, V. G. H. An oxidative enzyme boosting the enzymatic conversion of recalcitrant polysaccharides. *Science* **2010,** *330,* 219-222.
27. Quinlan, R. J.; Sweeney, M. D.; Leggio, L. L.; Otten, H.; Poulsen, J-C. N.; Johansen, K. S.; Krogh, K. B. R. M.; Jorgensen, C. I.; Tovborg, M.; Anthonsen, A.; Tryfona, T.; Walter, C. P.; Dupree, P.; Xu, F.; Davies, G. J.; Walton, P. H. Insights into the oxidative degradation of cellulose by a copper metalloenzyme that exploits biomass components. *PNAS*. **2011,** *108,* 15079-15084.
28. Couto, S. R.; Herrera, J. L. T. Industrial and biotechnological applications of laccases: a review. *Biotechnol. Adv.* **2016,** *24,* 500-513.
29. Bergqvist, C.; Ezzedine, K. Vitiligo: A Review. *Dermatology* **2020,** 1-22.
30. Halaban, R.; Svedine, S.; Cheng, E.; Smicun, Y.; Aron, R.; Hebert, D. N. Endoplasmic reticulum retention is a common defect associated with tyrosinase-negative albinism. *PNAS*. **2000,** *97,* 5889-5894.
31. Baldo, B. A. Enzymes approved for human therapy: indications, mechanisms and adverse effects. *BioDrugs* **2015,** *29,* 31-55.
32. Vellard, M. The enzyme as drug: application of enzymes as pharmaceuticals. *Curr. Opin. Biotech*. **2003,** *14,* 444-450.
33. Craik, C. S.; Page, M. J.; Madison, E. L. Proteases as therapeutics. *Biochem. J*. **2011,** *435,* 1-16.

34. Zhang, Q.; Chen, S.; Wang, H.; Yu, H. Exquisite enzyme-Fenton biomimetic catalysts for hydroxyl radical production by mimicking an enzyme cascade. *ACS Appl. Mater. Interfaces*. **2018**, *10*, 8666-8675.

35. Li, M.; Zhang, H.; Hou, Y.; Wang, X.; Xue, C.; Li, W.; Cai, K.; Zhao, Y.; Luo, Z. State-of-the-art iron-based nanozymes for biocatalytic tumor therapy. *Nanoscale Horizons*, **2020**, *5*, 202-217.

36. Wang, R.; Yan, C.; Zhang, H.; Guo, Z.; Zhu, W. H. In vivo real-time tracking of tumor-specific biocatalysis in cascade nanotheranostics enables synergistic cancer treatment. *Chem. Sci*. **2020**, *11*, 3371-3377.

37. Romero, O.; Filice, M.; de las Rivas, B.; Carrasco-Lopez, C.; Klett, J.; Morreale, A.; Hermoso, J. A.; Guisan, J. M.; Abian, O.; Palomo, J. M. Semisynthetic Peptide-Lipase Conjugates for Improved Biotransformations. *Chem.Commun*. **2012**, *72*, 9053-9055.

38. Lopez-Tejedor, D.; Palomo, J. M. Efficient purification of a highly active H-subunit of tyrosinase from Agaricus bisporus. *Protein Expr. Purif*. **2018,** *145*, 64-70.

39. Xie, W-Y.; Song, F.; Wang, X-L.; Wang, Y-Z. Development of Copper Phosphate Nanoflowers on Soy Protein toward a Superhydrophobic and Self-Cleaning Film. *ACS Sustainable Chem. Eng*. **2017**, *5*, 869−875.

40. Tan, X.; Wang, X.; Zhang, L.; Liu, L.; Zheng, G.; Li, H.; Zhou, F. Stable and Photothermally Efficient Antibody-Covered Cu3(PO4)2@Polydopamine Nanocomposites for Sensitive and Cost-Effective Immunoassays. *Anal. Chem*. **2019**, *91*, 13, 8274-8279.

41. Lawson, D. M.; Brzozowski, A. M.; Rety, S.; Verma, C.; Dodson, G. G. Probing the nature of substrate binding in Humicola lanuginosa lipase through X-ray crystallography and intuitive modelling. *PEDS*. **1994,** *7,* 543-550.

42. Durgadas, C. V.; Sharma, C. P.; Sreenivasan, K. Fluorescent gold clusters as nanosensors for copper ions in live cells. *Analyst* **2011,** *136,* 933-940.

43. Sicchieri, L. B.; Moreira Monteiro, A.; Samad, R. E.; Ito, A. S.; Figueiredo Neto, A. M.; Dias Vieira, N.; Gidlund, M.; Coronato Courrol, L. Study of tryptophan lifetime fluorescence following low-density lipoprotein modification. *Appl. Spectrosc*. **2013,** *67,* 379-384.

44. Ismaya, W.; Rozeboom, H. J.; Weijn, A.; Mes, J. J.; Fusetti, F.; Wichers, H. J.; Dijkstra, B. W. Crystal Structure of Agaricus bisporus Mushroom Tyrosinase: Identity of the Tetramer Subunits and Interaction with Tropolone. *Biochemistry* **2011,** *50,* 5477–5486.

45. Thawari, A. G.; Rao, C. P. Peroxidase-like catalytic activity of copper-mediated protein–inorganic hybrid nanoflowers and nanofibers of β-lactoglobulin and α-lactalbumin: synthesis, spectral characterization, microscopic features, and catalytic activity. *ACS Appl. Mater. Interfaces* **2016,** *8,* 10392-10402.

46. Lale, S. V.; Goyal, M.; Bansal, A. K. Development of lyophilization cycle and effect of excipients on the stability of catalase during lyophilization. *Int. J. Pharm. Investing.* **2011,** *1,* 214-221.

47. Sarbadhikary, P.; Dube, A. Iodinated chlorin p6 copper complex induces anti-proliferative effect in oral cancer cells through elevation of intracellular reactive oxygen species. *Chem-Biol Interact* **2017,** *277,* 137-144.

48. Mizutani, H.; Nishimoto, A.; Hotta, S.; Ikemura, K.; Imai, M.; Miyazawa, D.; Ohta, K.; Ikeda, Y.; Maeda, T.; Yoshikawa, M.; Hiraku, Y.; Kawanishi, S.

Oxidative DNA Damage Induced by Pirarubicin, an Anthracycline Anticancer Agent, in the Presence of Copper (II). *Anticancer Res*. **2018,** *38,* 2643-2648

49. Carrasco-López, C.; Godoy, C.; de las Rivas, B.; Fernández-Lorente, G.; Palomo, J. M.; Fernández-LaFuente, R.; Martínez-Ripoll, M.; Hermoso, J.A. Activation of bacterial thermoalkalophilic lipases is spurred by dramatic structural rearrangements. *J. Biol. Chem*. **2009,** *284,* 4365-4372.
50. Uppenberg, J.; Hansen, M. T.; Patkar, S.; Jones, T. A. The sequence, crystal structure determination and refinement of two crystal forms of lipase B from Candida antarctica. *Structure* **1994,** *2,* 293-308.
51. Zolghadri, S.; Bahrami, A.; Khan, M.T.H.; Munoz-Munoz, J.; Garcia-Molina, F.; Garcia-Canovas F.; Saboury, A.A. A comprehensive review on tyrosinase inhibitors. *J. Enzym. Inhib. Med. Ch.* **2019**, *34*, 279-309.
52. Zisis T.; Freddolino P.L; Turunen, P.; van Teeseling, M.C.F; Rowan, A.E.; Blank, K.G. Interfacial activation of Candida antarctica lipase B: combined evidence from experiment and simulation. *Biochemistry.* **2015**, *54*, 5969–5979.
53. Moreno-Pérez, S.; Ghattas, N.; Filice, M.; Guisan, J. M.; Fernandez-Lorente, G. Dramatic hyperactivation of lipase of Thermomyces lanuginosa by a cationic surfactant: Fixation of the hyperactivated form by adsorption on sulfopropyl-sepharose. *J. Mol. Catal. B: Enzym*. **2015**,*122*,199-203.

TOC GRAPHIC